Journal of Alloys and Compounds 473 (2009) 579–583

Contents lists available at ScienceDirect

Journal of Alloys and Compounds

journal homepage: www.elsevier.com/locate/jallcom

Synthesis, characterization and structure refinement of sodium zirconium molibdo-phosphate: $Na_{0.9}Zr_2Mo_{0.1}P_{2.9}O_{12}$ (MoNZP)

Rashmi Chourasia [a], O.P. Shrivastava [a,*], P.K. Wattal [b]

[a] Department of Chemistry, Dr. H.S. Gour University, C-65 Gour Nagar, University Campus, Sagar 470003, MP, India
[b] Back End Technology Development Division, Bhabha Atomic Research Center, Mumbai 400085, India

ARTICLE INFO

Article history:
Received 26 April 2008
Received in revised form 11 June 2008
Accepted 12 June 2008
Available online 19 August 2008

Keywords:
Ceramic
Zirconium phosphomolibdate
Powder XRD
Crystal structure refinement
Nuclear waste

ABSTRACT

Sodium zirconium phosphate (NZP) is a potential material for immobilization of nuclear effluent of reprocessing plants. The crystal structure of molybdenum containing NZP was determined on the basis of powder diffraction data by Rietveld method. It was found that molybdenum could be immobilized into NZP ceramic matrix without significant changes of the three-dimensional framework structure. The crystal chemistry of the title phase has been investigated using General Structure Analysis System (GSAS) programming. The MoNZP phase synthesized by ceramic route at 1050 °C crystallizes in the rhombohedral system (space group *R*-3*c*) with unit cell parameters: $a = b = 8.79255(11)$ Å, $c = 22.7495(5)$ Å and $Z = 6$. Step analysis of powder X-ray diffraction data has been subjected to Rietveld refinement to arrive at a satisfactory structural convergence of *R*-factors: $R_p = 0.0781$, $R_{wp} = 0.1051$ and $RF^2 = 0.06328$. The interatomic distances and bond angles are in good agreement with their standard values. The particle size along prominent reflecting planes calculated by Scherrer's formula ranges between 15 and 78 nm. The polyhedral distortions and valence calculations from bond strength data are also reported. Morphological examination by SEM reveals that the size of almost rectangular parallelepiped crystallites varies between 0.5 and 1.5 μm. The EDX analysis and IR spectroscopy provide analytical evidence of immobilization of molybdenum cation in the matrix.

1. Introduction

Reprocessing of spent nuclear power reactor fuel involves various steps such as solvent extraction of fission products, immobilization and final disposal of precipitate forming elements like Zr and Mo that cannot be concentrated by evaporation of liquid waste forms. It is therefore, desirable to understand crystallochemical fixation of Mo atoms into NZP like ceramic matrix for practical applications. The structural analogue of sodium zirconium phosphate (NZP) $NaZr_2(PO_4)_3$ is a potential material for immobilization of molybdenum from radio active waste along with other radio nuclides. The multicomponent material is a homogenous crystalline solid solution having desirable mechanical, physical and chemical stability. Apart from having good leach resistance, these materials are characterized by ultra low thermal expansion [1–3]. Due to the above-mentioned properties and structural flexibility of phosphates to incorporate large number of multivalent ions, NZP type ceramics could sustain 20–30% of waste loading through ceramic route of synthesis proposed for waste immobilization [4,5].

Till date, no detailed crystallographic model for immobilization of molybdenum in NZP has been reported. Apart from the relevance of technical feasibility of immobilization of multivalent transition metals in NZP matrix, the present investigation on molybdenum in which the valence of cation can be either +4 or +6, the scientific interest would be in the understanding of isomorphic substitution in to different positions of the same crystal structure and its relationship with chemical composition, structure and properties of the substances under consideration [6–11]. The mechanism of incorporation of molybdenum in the NZP solid solution has been explained by Pet'kov and Sukhanov [12–15]. Compounds of NZP family may be represented by the general crystal-chemical formula $(M1)(M2)_3\{[L_2(TO_4)_3]^{p-}\}_{3\infty}$. The structure consists of network of corner sharing LO_6 octahedrons and TO_4 tetrahedrons. The structural unit consisting of two octahedrons and three tetrahedrons $\{[L_2(TO_4)_3]^{p-}\}$ are connected in the form of ribbons parallel to the *c*-axis of the unit cell. These ribbons are linked together perpendicular to the *c*-axis by TO_4 tetrahedrons to build the three-dimensional framework. Molybdenum having different valences is reported to occupy either L or T positions in NZP framework [16–21]. Because Mo(IV) easily oxidizes in presence of air, it is difficult to fix Mo(IV) in L-type (Zr site) position of NZP structure, therefore fixing of Mo atoms in T-type positions would be a favorable study for effective

* Corresponding author. Tel.: +91 7582264249.
E-mail address: dr_ops11@rediffmail.com (O.P. Shrivastava).

0925-8388/$ – see front matter © 2008 Elsevier B.V. All rights reserved.
doi:10.1016/j.jallcom.2008.06.074

nuclear waste immobilization. The feasibility of substitution of Mo in place of equivalent P in T position of NZP structure was studied in the present investigation using Rietveld refinement of the simulated phase: $Na_{1-x}Zr_2(PO_4)_{3-x}(MO_4)_x$ where $x = 0.1$ (hereafter MoNZP).

2. Experimental

2.1. Ceramic route synthesis of MoNZP

MoNZP polycrystalline powder of the stoichiometry $Na_{0.9}Zr_2P_{2.9}Mo_{0.1}O_{12}$ was prepared from dry powders of Na_2CO_3, ZrO_2, $(NH_4)\cdot H_2PO_4$ and $(NH_4)_6Mo_7O_{24}\cdot 4H_2O$ as starting materials. The decomposition loss of MoO_3 was made up by addition of extra quantity of ammonium molibdate. The reagent grade chemicals have been thoroughly mixed with ~10 ml glycerol in a mortar–pestle. The glycerol paste was gradually heated initially at 600 °C for 8 h in a platinum crucible. This initial heating is done to decompose Na_2CO_3 and $(NH_4)H_2PO_4$ with emission of carbon dioxide, ammonia and water vapors. The mixture was reground to micron size, pressed into pellets and sintered in at 1050 °C for 72 h. The process was repeated to get a polycrystalline dense material.

2.2. Characterization

The powder X-ray diffraction pattern has been recorded between $2\theta = 10°$ and 90° on a Rigaku RUH3R diffractometer using Cu Kα radiation at step size of $2\theta = 0.02°$ and a fixed counting time of 2 s/step. The X-ray data was subjected to GSAS software, which is capable of handling and refining the step analysis diffraction data in a comprehensive manner. Scanning electron microscopy (SEM) has been carried out on a HITACHI S-3400n electron microscope system attached with Thermonoran ultra dry detector facility for energy dispersive X-ray (EDX) analysis. IR spectrum was recorded on SHIMADZU FT-IR spectrophotometer in the range of 500–4000 cm^{-1}. Sample was prepared by finely dispersing powder material on a KBr carrier.

3. Results and discussion

3.1. Crystallographic data and Rietveld refinement of the structure

The powder XRD data showed that a solid solution of $Na_{0.9}Zr_2P_{2.9}Mo_{0.1}O_{12}$ is formed which is isostructural to $NaZr_2(PO_4)_3$. MoNZP crystallizes in the rhombohedral system (space group *R*-3*c*). The conditions for the rhombohedral lattice: (i) $-h + k + l = 3n$, (ii) when $h = 0$, $l = 2n$ and (iii) when $k = 0$, $l = 2n$ have been verified for all reflections between $2\theta = 10°$ and 90°. The intensity and positions of the diffraction pattern match with the characteristic pattern of NZP, which give several prominent reflections between $2\theta = 13.98°$ and 46.47° [22]. The presence of ZrP_2O_7 phase in trace quantity have also been detected ($2\theta = 49.52°$ and IR ~746.48 cm^{-1}).The Rietveld refinement [23] of the step scan data was performed by the least square method using GSAS software [24]. Assuming that MoNZP belongs to the Nasicon family, Zr, P and O atoms are in the *12c*, *18e* and *36f* Wyckoff positions, respectively of the *R*-3*c* space group. Na atoms were assumed to occupy the M1 (6b) site. The occupancy of Na(1) was allowed to vary but the total P and Mo contents were constrained. The refinement leads to rather good agreement between the experimental and calculated XRD pattern (Fig. 1) and yields acceptable reliability factors: R_p, R_{wp} and RF^2 [25]. The normal probably plot for the histogram gives nearly a linear relationship indicating that the Io and Ic values for the most part are normally distributed.

The lattice parameters are close to the corresponding values for un-substituted NZP unit cell [26]. The cell parameters of the specimens register slight increase in the ***c*** direction. Simultaneously, the structure shows a slight contraction along *a* direction (Table 1). This is due to angular distortions as a result of the coupled rotation of ZrO_6 and PO_4 polyhedrons [27]. Alteration in lattice parameters shows that the network slightly modifies its dimensions to accommodate the cations occupying M1 and T sites without breaking the bonds. The basic framework of NZP accepts the cations of different sizes and oxidation states to form solid solutions but at

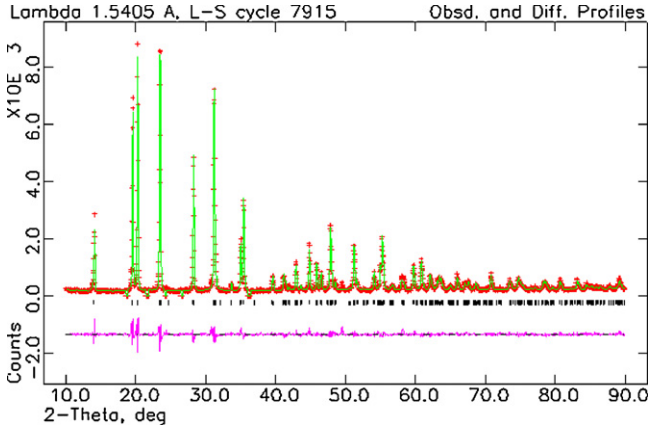

Fig. 1. Rietveld refinement pattern of MoNZP. The '+' are the raw X-ray diffraction data and the overlapping continuous line is the calculated pattern. Black vertical lines in the profile indicate the Bragg's positions of the allowed reflections for Cu Kα1 and Cu Kα2. The curve at the bottom is the difference in the observed and calculated intensities in the same scale.

Table 1
Crystallographic data for MoNZP at room temperature

Structure	Rhombohedral
Space group	*R*-3*c*
Lattice parameters	$a = b = 8.79255(11)$ Å, $c = 22.7495(5)$ Å, $\alpha = \beta = 90.0°$, $\gamma = 120.0°$
Z	6
R_p	0.0781
R_{wp}	0.1051
$R_{expected}$	0.0495
RF^2	0.06328
Volume of unit cell	1523.110(33) Å^3
S (GoF)	2.13
DWd	0.838
Unit cell formula weight	2980.410
$Density_{X\text{-}ray}$	3.249 g/cm^3
Slope	1.8139
No. of parameters refined	34

$R_p = \sum y_{i(o)} - y_{i(c)} / \sum y_{i(o)}$, $R_{wp} = \{\sum w_i(y_{i(o)} - y_{i(c)})^2 / \sum w_i(y_{i(o)})^2\}^2$, $R_e = [(N-P)/\sum w_i y_{oi}^2]^{1/2}$ $S = R_{wp}/R_{exp}$ $y_{i(o)}$ and $y_{i(c)}$ are observed and calculated intensities at profile point *i*, respectively. w_i is a weight for each step *i*. *N* and *P* shows the numbers of data and of refined parameters, respectively.

the same time retaining the overall geometry unchanged. The final atomic coordinates and isotropic thermal parameters (Table 2), inter-atomic distances and bond angles (Table 3), *h*, *k*, *l* values, *d*-spacing, intensity data along with observed and calculated structure factors generated by the crystal information file after final cycle of the Rietveld refinement. The refinement leads to acceptable Zr—O, P/Mo—O and Na—O bond distances. Zr atoms are displaced from the center of the octahedron due to the Na^+—Zr^{4+} repulsions. Consequently the Zr—O(7) distance (2.087 Å), neighboring the sodium Na(1), is slightly greater than the Zr—O(6) distance (2.059 Å). The average Zr—O distances (2.073 Å) are smaller than

Table 2
Refined atomic coordinates of MoNZP polycrystalline solid solution at room temperature

Atom	Wyckoff position	*x*	*y*	*z*	Occupancy	Uiso (Å^2)
Na1	6b	0.0	0.0	0.0	1.0	0.0426
Zr3	12c	0.0	0.0	0.146	1.0	0.02133
P4	18e	0.29078	0.0	0.25	0.968	0.03901
Mo5	18e	0.29078	0.0	0.25	0.03255	0.03901
O6	36f	0.1792	−0.03	0.1956	1.0	0.02906
O7	36f	0.1933	0.17	0.0874	1.0	0.02906

Table 3
Inter-atomic distances, bond angles and polyhedral distortions of polycrystalline MoNZP

Bond distances (Å)	
Na1_O7	2.556(4)*6
Zr3_O6	2.059(20)*3
Zr3_O7	2.087(30)*3
P4/Mo5_O6	1.518(20)*2
P4/Mo5_O7	1.530(20)*2
P4/Mo5_Na2	2.909(4)*2
P4/Mo5_Na2	3.070(4)
Na1_Zr3	3.321(8)*2
Angles (°)	
O7_Na1_O7	65.96(12)*6, 180.0(0)*2, 179.96(0), 114.03(12)*6
O6_Zr3_O6	92.84(10)*3
O7_Zr3_O7	83.59(11)*3
O6_Zr3_O7	92.31(10)*3, 90.88(10)*3, 173.46(0)
O6_P4_O6	111.97(14)
O6_P4_O7	104.55(10)*2, 113.40(6)*2
O7_P4_O7	109.13(0)
Polyhedral distortions (Å) $\#\Delta$ ($\times 10^4$)	
ZrO_6	16.90
PO_4	0.166

The * denotes multiplicity of bonds and angles The values in parentheses denote estimated values $\#\Delta = 1/n\Sigma\{(R_i - R_m)/(R_m)\}^2$ where $n = 4$, 6 and 8 for four, six and eight coordination, respectively.

the values calculated from the ionic radii data (2.12 Å) [28]. The O—Zr—O angles vary between 83.59° and 173.46°. The angles implying the shortest bonds are superior to those involving the longest ones due to O—O repulsions which are stronger for O(6)—O(6) than for O(6)—O(7).

The P—O distances (in pairs) 1.518 and 1.530 Å are close to those found in Nascicon type phosphates [29]. The O—P—O angles vary between 104.55° and 113.40°. The Na(1) atoms occupy the center of the M1 site. The six coordinate Na(1)—O(7) bond is 2.556 Å. PLATON projection of the molecular structure shows that the inter-linking of $Zr(3)O_6$ and $P(4)O_4$ takes place through a bridge oxygen atom. Fig. 2 illustrates the DIAMOND view showing the ZrO_6 inter-ribbon distance in the structure of the title phase, which is a function of amount and size of alkali cation in the M site of the 3D framework, built from ZrO_6 octahedrons and corner sharing PO_4 tetrahedrons. The polyhedral distortions (Δ) [30,31] in the ZrO_6 and PO_4 reported

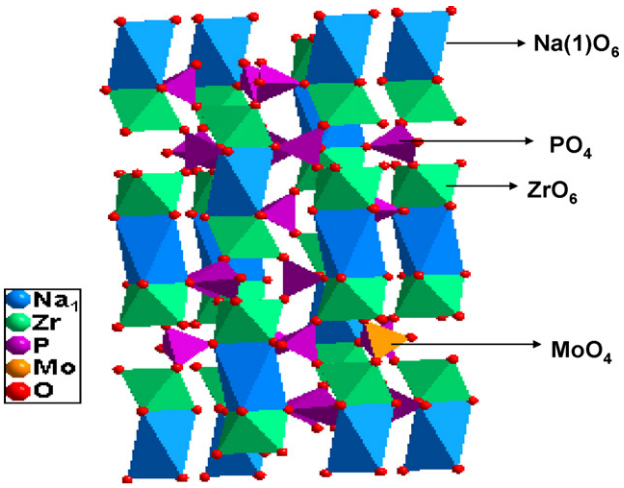

Fig. 2. DIAMOND view of coordination sites of Na, Zr and P/Mo in MoNZP.

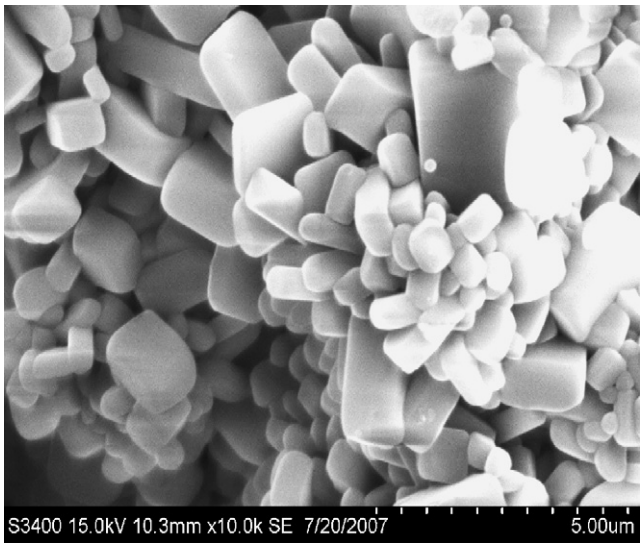

Fig. 3. Scanning electron micrograph of MoNZP ceramic powder synthesized at 1050 °C.

in Table 3 are found as 1.690×10^{-3} and 1.66×10^{-5} Å, respectively. The calculated valences $V_i = \Sigma b_{ij}$ [where $b_{ij} = (R_o/R)^N$] based on bond strength analysis [32–34] are as follows—Na(1): 0.852, Zr: 4.23, P: 5.22 .These values are close to the expected formal oxidation states of Na^+, Zr^{4+} and P^{5+}, respectively.

3.2. SEM and EDX analysis

The microstructure of the title phase has been examined by SEM and EDX analysis of the specimen. The evolution of MoNZP phase can be seen clearly in the electron micrographs of the ceramic sample, which has explicit parallelepiped grains of size 0.5–1.5 μm (Fig. 3). Within the limits of experimental error, the EDX analytical data on atomic and wt.% of Na, Zr, P and Mo are found agreeable with their corresponding expected molar ratios. The EDX spectrum shows that molybdenum crystallochemically enters the NZP matrix (Fig. 4).

3.3. Infrared spectra

The presence of orthophosphate and orthomolybdate anions was confirmed by their characteristic IR bands due to stretching and bending vibrations of P—O bonds of PO_4 tetrahedron. In the spectra,

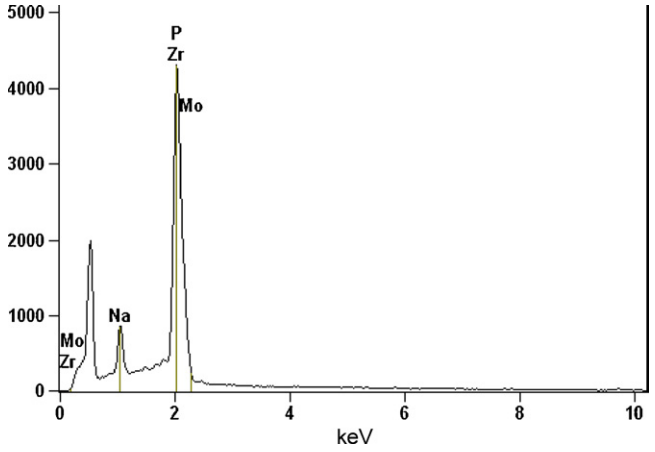

Fig. 4. EDAX spectrum of polycrystalline MoNZP ceramic material.

Table 4
Distribution of particle size along prominent reflecting planes of MoNZP ceramic sample

hkl	FWHM (2θ)	Particle size (nm)
10–2	0.14	78.12
104	0.16	53.00
110	0.16	65.82
006	0.16	74.15
202	0.26	31.27
20–4	0.20	40.99
116	0.20	41.28
10–8	0.34	24.23
214	0.22	37.76
300	0.18	46.30
21–5	0.22	37.93
208	0.26	32.17
119	0.54	15.65
30–6	0.24	35.39
21–8	0.24	35.48
31–4	0.26	32.85
20–10	0.32	26.87
226	0.26	33.20

two main regions can be identified in the range 1300–400 cm^{-1} that are attributed to the phosphate unit: (1) the bands between 1250 and 900 cm^{-1} are ascribed to the stretching vibrations of the PO_4 unit (ν_1 and ν_3 modes), (2) the bands between 650 and 400 cm^{-1} are due to the deformation of the O—P—O angle (ν_2 and ν_4 modes). A broad band in 897 cm^{-1} is attributed to asymmetric vibrations of MoO_4 tetrahedron (Fig. 5) [35,36].

3.4. Particle size distribution

The X-ray diffraction data of MoNZP sample was used for the estimation of particle size using Scherer's formula [37,38]. The *h*, *k*, *l* values corresponding to prominent reflections, full width at the half intensity of maxima (FWHM) and particle size for crystals are shown in Table 4 The particle size distribution along the prominent reflecting planes mentioned in table ranges between 15 and 78 nm for the title phase.

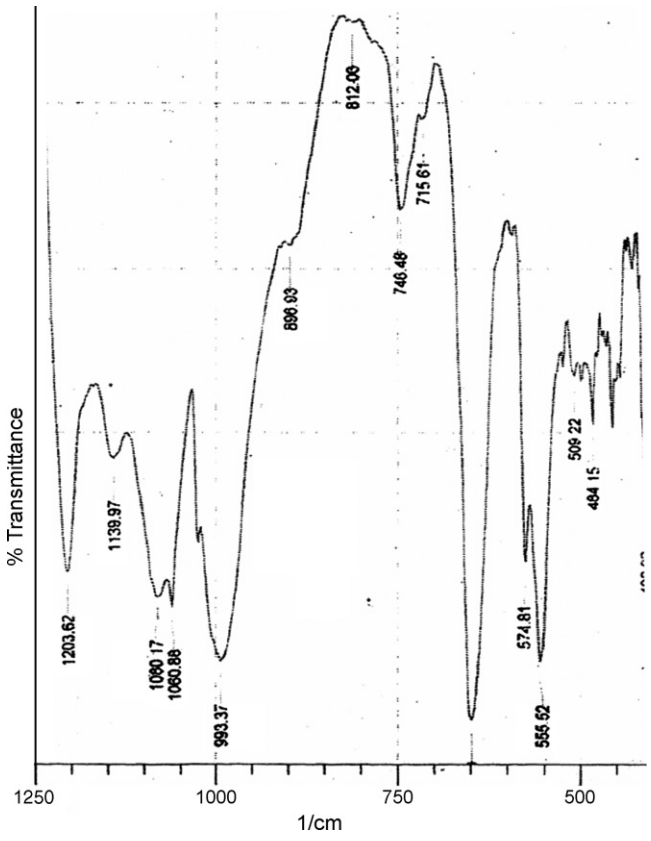

Fig. 5. Infrared spectra of MoNZP ceramic sample.

3.5. Electronic charge distribution

The chemical bonding mechanism has been studied on the basis of electronic charge density. Fig. 6 shows the contour maps of the charge density in the molecular framework. At the center

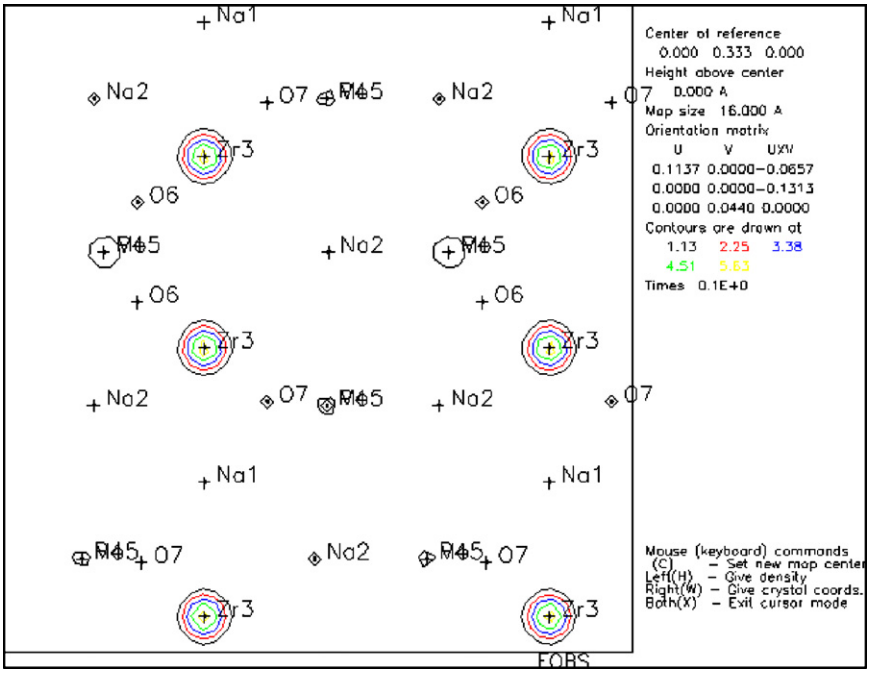

Fig. 6. Calculated Fourier map showing contours of charge density of Zr, P/Mo and other atoms of MoNZP.

of Zr atoms, the charge density maxima are between 6.08 and 6.34 a.u.^{3}. There are two charge density minima for the two bond distances (2.027 and 2.066 Å) between Zr and O atoms, i.e. 0.014 and 0.065 electron per a.u.^{3}. The Zr—O bond is covalent with some degree of ionic character due to hybridization effect between Zr-*4d* and O-*2p* states [39]. Similarly, there are two charge density minima for two types of P—O bond lengths (1.521 and 1.533 Å). The charge density ratios at the center of the Zr and P atoms of various contours vary from a low of 3.19 to a high charge density of 4.54 against the expected value of 3.6.

4. Conclusion

Refinement of powder X-ray diffraction data shows that the solid solutions of Mo substituted NZP crystallize in the rhombohedral (*R*-3*c* space group) system. The structure refinement suggests that hexavalent Mo partially substitute phosphorus (T site) and the resultant charge compensation takes place though sodium ions. Crystal data and structural parameters of the material have been refined to a satisfactory convergence with reasonable values of Rietveld parameters (R_p and R_{wp}). The calculated values of P—O and Zr—O bond lengths and O—M—O bond angles are in agreement with the expected values. The NZP has been identified as a potential material for immobilization and solidification of molybdenum. Analytical evidence has been found to conclude that the molybdenum is crystallochemically fixed in the ceramic matrix.

Acknowledgements

The authors thankfully acknowledge the financial assistance received from the Department of Science and Technology, Govt. of India, New Delhi for funding the research project no. SR/S3/ME/20/2005-SERC-Engg under its SERC scheme. We also thank the director of UGC–DAE consortium for scientific research Indore, India for providing X-ray facility and Department of Metallurgical Engineering and Materials IIT Mumbai, India for SEM/EDX analysis.

References

[1] V.I. Petkov, A.I. Orlova, Inorg. Mater. 39 (10) (2003) 1013–1023.
[2] J. Alamo, R. Roy, J. Mater. Sci. 21 (1986) 444.
[3] P. Oikonomou, Ch. Dedeloudis, C.J. Stournaras, Ch. Ftikos, J. Eur. Ceram. Soc. 27 (2007) 1253–1258.
[4] B.E. Scheetz, D.K. Agrawal, E. Breval, Waste Manage. 14 (1994) 489.
[5] I.W. Donald, B.L. Metcalfe, R.N.J. Taylor, J. Mater. Sci. 32 (1997) 5851.
[6] Y. Miyajima, T. Miyoshi, J. Tamaki, M. Matsuoka, Y. Yamamoto, C. Masquelier, M. Tabuchi, S. Yuria, Solid State Ionics 124 (1999) 201–211.
[7] Y. Hirose, T. Fukasawa, D.K. Agrawal, B.E. Scheetz, R. Nageswaran, J.A. Curtis, S.Y. Limaye, WM 1999 Conference, 1999.
[8] C. Delmas, A. Nadiri, J.L. Sobeyroux, Solid State Ionics 28–30 (1988) 419.
[9] J.M. Winand, A. Rulmont, P. Tarte, Solid State Ionics 39 (1991) 341.
[10] J.L. Rodrigo, J. Alamo, Mater. Res. Bull. 26 (1991) 475.
[11] J. Alamo, J.L. Rodrigo, Mater. Res. Bull. 27 (1992) 1091.
[12] V.I. Pet'kov, M.V. Sukhanov, Czech. J. Phys. 53 (2003) A671–A677.
[13] V.I. Pet'kov, G.I. Dorokhova, A.I. Orlova, Crystallogr. Rep. 46 (2001) 69.
[14] V.I. Pet'kov, M.V. Sukhanov, V.S. Kurazhkovskaya, Radiochemistry 45 (2003) 620–625.
[15] M.V. Sukhanov, V.I. Pet'kov, V.S. Kurazhkovskaya, N.N. Eremin, V.S. Urusov Russian, J. Inorg. Chem. 51 (2006) 706–711.
[16] Z.I. Khazheeva, et al., Kristallografiya 32 (1987) 79.
[17] B.I. Lazoriak, V.A. Efremov, Zhurn. Neorgan. Khimii. 32 (1987) 652.
[18] A. Leclaire, M.M. Borel, A. Grandin, B. Raveau, Eur. J. Solid State Inorg. Chem. 26 (1989) 45.
[19] K.H. Lii, J.J. Chen, S.L. Wand, J. Solid State Chem. 78 (1989) 93.
[20] L. Bennouna, et al., J. Solid State Chem. 114 (1995) 224.
[21] N.M. Kozhevnikova, I. Yu Kotova, Rus. J. Inorg. Chem. 45 (2000) 96.
[22] JCPDS Powder diffraction data file no. 71-0959, compiled by International Center for Diffraction Data U.S.A., 2000.
[23] H.M. Rietveld, Acta Crystallogr. 2 (1969) 65.
[24] A.C. Larson, R.B. Von Dreele, General Structure Analysis System Technical Manual LANSCE, MS-H805, Los Almos National University LAUR, 2000, pp. 86–748.
[25] H. Kojitani, M. Kido, M. Akaogi, Phys. Chem. Miner. 32 (2005) 290–294.
[26] M.S. Verissimo Carla, L. Garrido Francisco, O. Alves, P. Calle, Martinez Juarez Ana, E. Iglesias Juan, M. Rojo Jose, Solid State Ionics 100 (1997) 127–134.
[27] K.V. Govindan Kutty, R. Asuvathraman, R. Sridhran, J. Mater. Sci. 33 (1998) 4007–4013.
[28] R.D. Shannon, Acta Crystallogr. A 32 (1976) 751.
[29] M. Chakir, A. El Jazouli, D. de Waal, J. Solid State Chem. 179 (2006) 1883–1891.
[30] H. Mitchell Roger, P. Liferovich, J. Ruslan, Solid State Chem. 177 (2004) 4420–4427.
[31] O.P. Shrivastava, R. Chourasia, J. Chem. Crystallogr. 38 (2008) 357–362.
[32] A.R. West, Solid State Chemistry and its Application, John Willey and Sons, Singapore, 2003, p. 710, chapter A9.
[33] N.E. Brese, M. O'Keeffe, Acta Crystallogr. B 47 (1976) 751.
[34] I.D. Brown, R.D. Shannon, Acta Crystallogr. A29 (1973) 266.
[35] J.B. Frank, N. Costantini, E.S. Lesley, Solid State Ionics 177 (2006) 2889–2896.
[36] G. Buvaneswari, U.V. Varadaraju, J. Solid State Chem. 145 (1999) 227–234.
[37] N. Bhatt, R. Vaidya, S.G. Patel, A.R. Jani, Bull. Mater. Sci. 27 (2004) 23–25.
[38] O.P. Shrivastava, R. Chourasia, J. Hazard. Mater. 153 (2008) 285–292.
[39] R. Terki, G. Bertrand, G.H. Aourag, Microelectr. Eng. 81 (2005) 514–523.